Journal of Hazardous Materials 190 (2011) 480–485

Contents lists available at ScienceDirect

Journal of Hazardous Materials

journal homepage: www.elsevier.com/locate/jhazmat

Electrochemical detection of DNA damage induced by acrylamide and its metabolite at the graphene-ionic liquid-Nafion modified pyrolytic graphite electrode

Yanyan Qiu, Xiangjin Qu*, Jing Dong, Shiyun Ai*, Ruixia Han

College of Chemistry and Material Science, Shandong Agricultural University, Daizong Street 61, Taian 271018, Shandong, China

ARTICLE INFO

Article history:
Received 19 November 2010
Received in revised form 17 March 2011
Accepted 21 March 2011
Available online 29 March 2011

Keywords:
Electrochemical detection
DNA damage
Acrylamide
Horseradish peroxidase
Layer-by-layer

ABSTRACT

A new electrochemical biosensor for directly detecting DNA damage induced by acrylamide (AA) and its metabolite was presented in this work. The graphene-ionic liquid-Nafion modified pyrolytic graphite electrode (PGE) was prepared, and then horseradish peroxidase (HRP) and natural double-stranded DNA were alternately assembled on the modified electrode by the layer-by-layer method. The PGE/graphene-ionic liquid-Nafion and the construction of the $(HRP/DNA)_n$ film were characterized by electrochemical impedance spectroscopy. With the guanine signal in DNA as an indicator, the damage of DNA was detected by differential pulse voltammetry after PGE/graphene-ionic liquid-Nafion/$(HRP/DNA)_n$ was incubated in AA solution or AA + H_2O_2 solution at 37 °C. This method provides a new model to mimic and directly detect DNA damage induced by chemical pollutants and their metabolites in vitro. The results indicated that, in the presence of H_2O_2, HRP was activated and catalyzed the transformation of AA to glycidamide, which could form DNA adducts and induce more serious damage of DNA than AA. In order to further verify these results, UV–vis spectrophotometry was also used to investigate DNA damage induced by AA and its metabolites in solution and the similar results were obtained.

1. Introduction

Acrylamide (AA), an α,β-unsaturated carbonyl compound, has been produced since the early 1950s. It has been widely used in various industrial fields like polymers, concretes, water treatment and paper industry. AA is well known for its neurotoxicity, genotoxicity and reproductive toxicity in experimental animals [1]. And the International Agency for Research on Cancer has classified it as a probable human carcinogen (group 2A) [2]. Under ordinary circumstances, humans are rarely exposed to AA and the concern about AA was centered only on occupational exposure. However, in 2000 AA was unexpectedly discovered in many common starchy foods [3], which may be formed during frying and baking through the Maillard reaction. Moreover, the carcinogenicity of AA was also demonstrated in human cells [4]. Therefore, the discovery of acrylamide in our daily diet has focused the world's attention on the public health problem.

DNA damage induced by chemical pollutants is a major endogenous toxicity pathway in biological system [5]. In the presence of a metabolic activation system, acrylamide is metabolized by the epoxidation of cytochrome P450 into its epoxide, glycidamide [6,7], which is considered to be mainly responsible for the carcinogenic activity of AA in vivo [8]. Cytochrome P450, a heme enzyme expressed in human liver microsomes, plays an important role in the metabolism of drugs, pollutants, and other foreign compounds. It catalyzes a diversity of chemical reactions such as epoxidation, hydroxylation and heteroatom oxidation [9]. The epoxidation of styrene catalyzed by cytochrome P450 to styrene oxide has been widely investigated [10,11]. Recently, Zu [12] firstly reported HRP/H_2O_2 was used to mimic cytochrome P450 for metabolizing styrene and the same product was obtained. It indicated that HRP/H_2O_2 played a similar role with cytochrome P450 in the metabolism and bioactivation, especially in epoxidation. Moreover, it also has been widely reported that HRP/H_2O_2 was used to mimic cytochrome P450 in metabolism and biotransformation [13,14]. Therefore, in our work, HRP/H_2O_2 enzyme system as an alternative to cytochrome P450 was used to metabolize AA for investigating DNA damage.

Electrochemical methods have been widely used as an in vitro model system to mimic the pathway of DNA damage in real bioprocess. Rusling's group has reported an enzyme-DNA biosensor which was used to detect DNA damage after enzyme-catalyzed bioactivation of a carcinogenic chemical styrene [15]. In their work, with electroactive Ru(II) complexes as the catalysts for guanine bases

* Corresponding authors. Tel.: +86 538 8247660; fax: +86 538 8242251.
E-mail addresses: xwp@sdau.edu.cn (X. Qu), ashy@sdau.edu.cn (S. Ai).

0304-3894/$ – see front matter © 2011 Elsevier B.V. All rights reserved.
doi:10.1016/j.jhazmat.2011.03.071

and external indicator, DNA damage induced by carcinogens was indirectly detected through the electrochemical signal changes of Ru(II) complexes [16].

Electrode modified material is very important in the design and application of modified electrodes and plays a critical role in the electrochemical sensing and biosensing. Graphene, a "rising star" nanostructured carbon material, is a single layer of sp^2 hybridized carbon atoms with a hexagonal arrangement in a two-dimensional lattice [17]. Due to the unique sheet structure, graphene displays intriguing attributes, such as fast electron transportation, high thermal conductivity, excellent mechanical stiffness and good biocompatibility [18]. Recently, it has received considerable interests for potential applications in nanocomposites [19], electrochemical sensors [20] and electrocatalysis [21]. Zhou [22] reported that graphene possessed excellent electrochemically catalytic property towards guanine bases of DNA, which indicated the potential applications of graphene in the label-free electrochemical detection of DNA hybridization and DNA damage. Based on this point, graphene was used as electrode modified material to prepare the biosensor and directly detect DNA damage without any other external indicator in our work.

However, graphene sheets tend to form irreversible agglomerates through strong π–π stacking and van der Waals interaction, which limits their further biological applications [23]. Especially as an electrode modified material, it is vitally important to prevent the aggregation of graphene sheets because most of their unique properties are associated with individual sheets. Herein, in order to solve this problem, Nafion was used to disperse graphene in aqueous solution as previously reported [24]. Besides, ionic liquid (IL) was also used as an electrode modified material in our work due to its high ionic conductivity, good stability and well biocompatibility [25].

In this paper, graphene was dispersed in Nafion solution to form a homogenous mixture of graphene–Nafion. In order to improve the conductivity, IL was doped into the mixture and the graphene-IL-Nafion nanocomposite was obtained. With the isoelectric point at 8.9 [26], HRP has net positive surface charges at pH 5.5 phosphate buffer solutions. Based on this point, positively charged HRP and negatively charged DNA were assembled on the graphene-IL-Nafion modified pyrolytic graphite electrode (PGE) by electrostatic attraction. The graphene-IL-Nafion nanocomposites provide a negatively charged surface for the immobilization of HRP and a biocompatible microenvironment to retain its bioactivity. After PGE/graphene-IL-Nafion/$(HRP/DNA)_n$ was incubated in AA or AA + H_2O_2 at 37 °C, DNA damage was detected by differential pulse voltammetry (DPV) based on the oxidation signal of guanine without any other external indicator. This method of directly detecting DNA damage provides a new strategy to screen the genotoxicity of new chemical pollutants and drugs in vitro. As far as we know, there are no reports on direct electrochemical detection of DNA damage induced by AA and its metabolite at PGE/graphene-IL-Nafion/$(HRP/DNA)_n$.

2. Experimental

2.1. Chemicals and apparatus

Double-stranded deoxyribonucleic acid sodium salt of calf thymus (dsDNA) was purchased from Sigma and used as received. HRP was obtained from Beijing Solarbio Science & Technology Co., Ltd. Graphene was synthesized according to previous report [27]. Briefly, graphite powder was reacted with concentrated H_2SO_4, $K_2S_2O_8$, and P_2O_5 at 80 °C for 6 h. After that, the mixture was diluted with deionized water, filtered with 0.2 μm Nylon film and dried naturally. The product was reoxidized with concentrated H_2SO_4 and $KMnO_4$ and graphite oxide was obtained. In order to exfoliate graphite oxide, 0.1 mg/mL graphite oxide dispersion was sonicated for 1 h. And then, appropriate hydrazine was added into the above solution and kept stirring for 24 h at 50 °C. Finally, black hydrophobic graphene was obtained by filtration and dried in vacuum. 0.1% Nafion solution was prepared by diluting the standard Nafion solution with doubly distilled water. 1-Ethyl-3-methylimidazolium ethylsulfate (IL) was purchased from Cheng Jie Chemical Co., Ltd. (Shanghai, China). 30% H_2O_2 solution was purchased from Shanghai Lingfeng Chemical Reagent Co., Ltd., and a fresh solution of H_2O_2 was prepared daily. 0.1 M phosphate buffer solutions (PBS) of pH 5.5 and pH 7.0 were prepared by mixing the stock solutions of 0.1 M NaH_2PO_4 and 0.1 M Na_2HPO_4. All other chemicals were of analytical grade and used as received. Doubly distilled water was used for all the preparations.

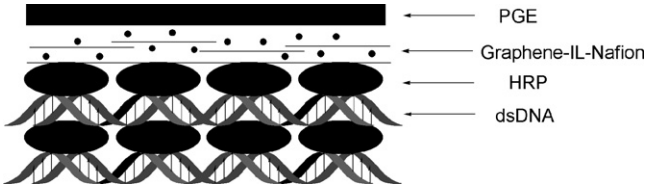

Scheme 1. Schematic diagram of PGE/graphene-Nafion-IL/$(HRP/DNA)_n$.

All the electrochemical measurements were performed on a CHI660C electrochemical workstation (Shanghai CH Instrument Company, China). A conventional three-electrode system was used with a bare or modified PGE (4 mm in diameter) as working electrode, a saturated calomel electrode (SCE) as reference electrode and a platinum wire as auxiliary electrode. All potentials given in this paper were referred to SCE. The transmission electron microscope (TEM) image was obtained at JEOL-1200 EX with accelerating voltage of 80 kV (Japan). Ultraviolet and visible (UV–vis) absorption spectrums were obtained using a Shimadzu UV-2450 spectrophotometer (Japan) at room temperature.

2.2. Preparation of modified electrode

The PGE was first polished to a mirror-like surface with 0.3 and 0.05 μm alumina slurry, and then sonicated successively in absolute alcohol and doubly distilled water. Finally, the PGE was dried at room temperature for further use.

In order to prepare the modified electrode, 0.6 mg graphene was dispersed in 2 mL 0.1% Nafion solution with ultrasonication for 2 h to form a homogenous mixture of graphene–Nafion. And then, 10 μL of IL was added into graphene–Nafion solution, and continuously sonicated to obtain a homogenous graphene-IL-Nafion solution. 6 μL of graphene-IL-Nafion solution was droped on the fresh prepared PGE surface and dried at room temperature. After that, 3.5 μL HRP solution (2.0 mg mL^{-1}, pH 5.5) and 4 μL dsDNA solution (1.0 mg mL^{-1}, pH 7.0) were alternately coated on the graphene-IL-Nafion modified PGE. Each layer was gently rinsed with doubly distilled water to remove weakly adsorbed molecules and dried at 4 °C in a refrigerator. In order to assemble $(HRP/DNA)_n$ layer-by-layer films on PGE/graphene-IL-Nafion, this adsorption cycle was repeated to the desired bilayer number (n). The obtained electrode was noted as PGE/graphene-IL-Nafion/$(HRP/DNA)_n$. The schematic diagram of PGE/graphene-IL-Nafion/$(HRP/DNA)_n$ was shown in Scheme 1. The modified electrode was kept at 4 °C in the dark before use.

2.3. Electrochemical measurements

For electrochemical detection of DNA damage induced by AA and its metabolite, the PGE/graphene-IL-Nafion/$(HRP/DNA)_n$ was

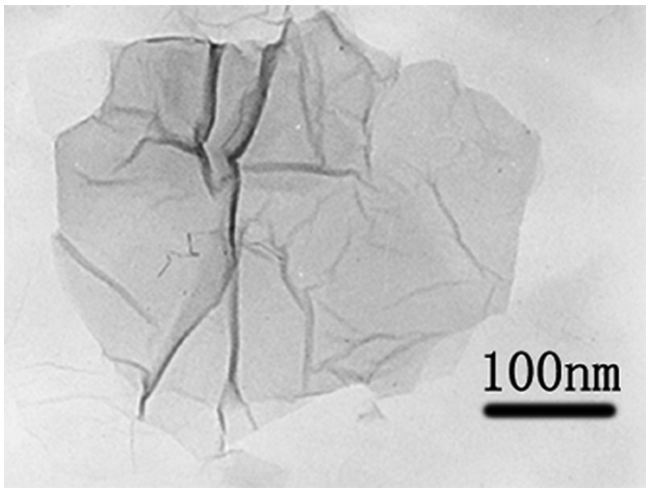

Fig. 1. TEM image of graphene–Nafion.

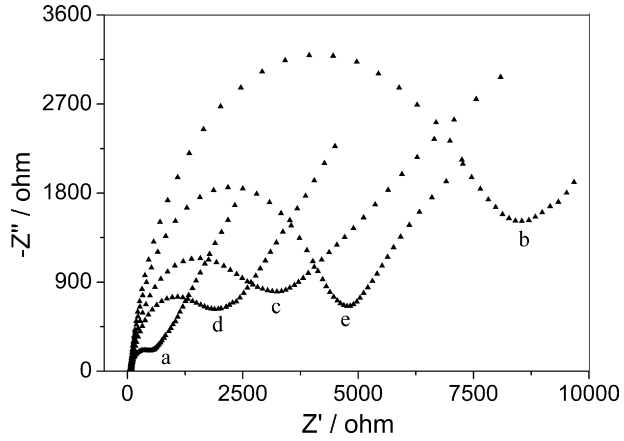

Fig. 2. Electrochemical impedance spectroscopies of PGE (a), PGE/Nafion (b), PGE/graphene–Nafion (c), PGE/graphene-IL-Nafion (d) and PGE/graphene-IL-Nafion/$(HRP/DNA)_n$ (e) in 5 mM $K_3[Fe(CN)_6]/K_4[Fe(CN)_6]$ (1:1) solution containing 0.1 M KCl.

incubated in pH 5.5 PBS containing 0.1% AA or 0.1% AA + H_2O_2 at 37 °C. After that, the modified electrode was transferred into the blank pH 7.0 PBS and DNA damage was detected by DPV using the guanine signal in DNA as an indicator. As a control experiment, the PGE/graphene-IL-Nafion/$(HRP/DNA)_n$ was incubated in blank buffers under the same condition and then used for electrochemical measurements.

2.4. UV–vis spectrophotometry

UV–vis spectrophotometry was also used to investigate DNA damage induced by AA and its metabolite in this work. The characteristic absorption of DNA at 260 nm was used as an indicator of DNA damage. After DNA (16 μg/mL) and 0.1% AA or 1 μg/mL HRP + 0.5 mM H_2O_2 + 0.1% AA were incubated for 12 h, UV–vis absorption spectrum was obtained using the corresponding DNA blank as a reference solution. In order to investigate the effect of other factors on DNA damage, UV–vis absorption spectrums of DNA were also recorded after DNA was incubated with HRP, H_2O_2 and HRP + H_2O_2 respectively under the same conditions.

3. Results and discussion

3.1. Characterization of graphene–Nafion by TEM

The graphene–Nafion was characterized by TEM and the result was shown in Fig. 1. As most unique properties of graphene are dependent on its individual sheet structure, it is important to preserve the morphology of graphene for the electrochemical performance. The TEM image of graphene–Nafion showed a general view of graphene nanoplatelets. It clearly illustrated graphene nanoplatelets were transparent and flake-like.

3.2. Electrochemical characterization of PGE/graphene-IL-Nafion/$(HRP/DNA)_n$

Electrochemical impedance spectroscopy (EIS), as a high effective method, was used to probe the surface features of modified electrodes and confirm the assembly of $(HRP/DNA)_n$ (when $n = 1$) films in this work. Fig. 2 shows the Nyquist plots of different modified electrodes in 5 mM $K_3[Fe(CN)_6]/K_4[Fe(CN)_6]$ (1:1) solution containing 0.1 M KCl. As shown in Fig. 2a, there was a small well-defined semicircle at high frequencies region obtained at the bare PGE, indicating small interface impedance. After coated with Nafion (Fig. 2b), the impedance values increased obviously. It could be attributed to the negatively charged skeleton of Nafion that blocked the diffusion of $[Fe(CN)_6]^{3-/4-}$ into the film and hindered the electron transfer [28]. However, the interface electron resistance decreased remarkably at PGE/graphene–Nafion (Fig. 2c), indicating that graphene as the conducting bridges promoted the electron transfer of $[Fe(CN)_6]^{3-/4-}$. After IL was doped in graphene–Nafion, the further decrease of interface electron resistance was observed as shown in Fig. 2d, which could be due to the high ionic conductivity of IL [29]. After positively charged HRP and negatively charged DNA were alternatively adsorbed on the surface of PGE/graphene-IL-Nafion, an obvious increase in the interface impedance was observed in Fig. 2e. It could be ascribed to the negatively charged DNA in the (HRP/DNA) film, which blocked the electron transfer of $[Fe(CN)_6]^{3-/4-}$ with negative charge. Meanwhile, it also suggested that the (HRP/DNA) film was successfully immobilized on the PGE/graphene-IL-Nafion.

3.3. Optimization of the bilayer number (n) of HRP/DNA

Electrochemical impedance spectroscopies of different HRP/DNA bilayers assembled on PGE/graphene-IL-Nafion were obtained in 5 mM $K_3[Fe(CN)_6]/K_4[Fe(CN)_6]$ (1:1) solution containing 0.1 M KCl and the related results were shown in Fig. 3. Upon the stepwise multilayer formation, it became more and more difficult for $[Fe(CN)6]^{3-/4-}$ to access the electrode surface. The increase of charge transfer resistance was consistent with the deposition of each sequential bilayer, which provided the evidence of HRP/DNA formation [30]. As can be seen in inset of Fig. 3, with the increase of the bilayer number (n) of HRP/DNA, the Ret values grew up to $n = 3$ almost in linear mode, and then did not increase linearly with n anymore. This phenomenon indicated that the $(HRP/DNA)_n$ films were successfully assembled on the surface of PGE/graphene-IL-Nafion at least when $n < 4$. Furthermore, the Ret value was proportional to the number of HRP/DNA bilayers, which illustrated that the multiplayer films were uniformly formed when $n < 4$. Therefore, this adsorption cycle of HRP/DNA at the PGE/graphene-IL-Nafion was repeated to three layers in our work.

3.4. Electrochemical detection of DNA damage on PGE/graphene-IL-Nafion/$(HRP/DNA)_3$

Electrochemical detection of DNA damage induced by acrylamide and its metabolite was investigated at the graphene-IL-Nafion/$(HRP/DNA)_3$ modified PGE. Fig. 4 shows differential pulse voltammograms of the modified electrode after incubated in

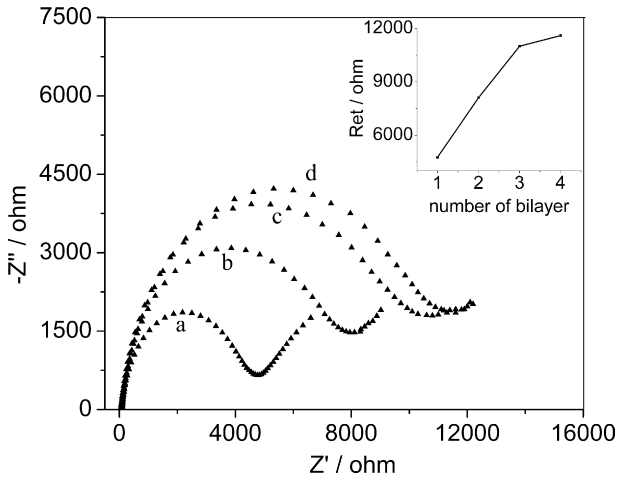

Fig. 3. Electrochemical impedance spectroscopies of PGE/graphene-IL-Nafion/(HRP/DNA)$_n$ with the increasing number of (HRP/DNA) bilayer from n = 1 to 4 (shown from a to d) in 5 mM $K_3[Fe(CN)_6]/K_4[Fe(CN)_6]$ (1:1) solution containing 0.1 M KCl. Inset: relationship of the electron transfer resistance (Ret) with the number of (HRP/DNA) bilayer.

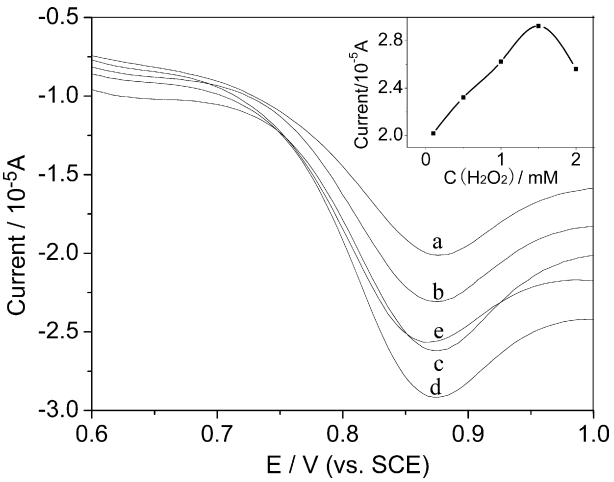

Fig. 5. Differential pulse voltammograms of PGE/graphene-IL-Nafion/(HRP/DNA)$_3$ in pH 5.5 PBS containing 0.1% AA + H_2O_2 with different concentrations of H_2O_2: (a) 0.1 mM, (b) 0.5 mM, (c) 1 mM, (d) 1.5 mM and (e) 2 mM. Inset is the relationship between the concentration of H_2O_2 and the peak current of guanine.

different solutions. As can be seen in Fig. 4a, there was no remarkable oxidation signal at PGE/graphene-IL-Nafion/(HRP/DNA)$_3$ after incubated in the blank solution. A similar result was obtained after the PGE/graphene-IL-Nafion/(HRP/DNA)$_3$ was incubated in H_2O_2 solution as shown in Fig. 4b. The possible reason for this phenomenon was that the active bases were protected by the double-stranded form of DNA and the electron transfer became very difficult to reach the electrode surface [31]. At the same time, it also demonstrated that DNA maintained the intact double helix under these two conditions. When the modified electrode was incubated in pH 5.5 PBS containing 0.1% AA or 0.1% AA + 1.5 mM H_2O_2 (Fig. 4c and d), there was an obvious peak at 0.87 V corresponding to guanine oxidation, which could be explained that the double helix of DNA was disturbed or destroyed during the incubation. These changes of DNA structure resulted from DNA damage. Upon comparison of Fig. 4c and d, the graphene-IL-Nafion/(HRP/DNA)$_3$ modified PGE exhibited larger peak current at 0.87 V after incubation in 0.1% AA + 1.5 mM H_2O_2 solution than that in 0.1% AA solution. It indicated that DNA damage in AA + H_2O_2 solution was larger than that in AA solution.

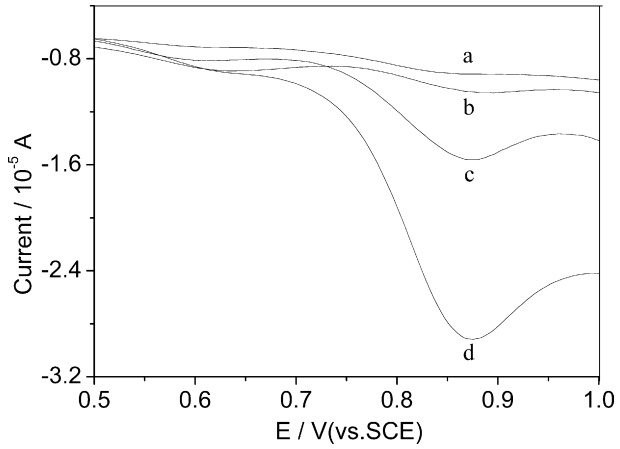

Fig. 4. Differential pulse voltammograms of PGE/graphene-IL-Nafion/(HRP/DNA)$_3$ in pH 7.0 PBS after incubation in pH 5.5 PBS containing: (a) blank; (b) 1.5 mM H_2O_2; (c) 0.1% AA and (d) 0.1% AA + 1.5 mM H_2O_2.

3.5. *Effect of H_2O_2 on the HRP activity*

In order to investigate the effect of H_2O_2 on the HRP activity, PGE/graphene-IL-Nafion/(HRP/DNA)$_3$ was incubated in pH 5.5 PBS containing 0.1% AA + H_2O_2 with different concentrations of H_2O_2 and the related data were recorded as shown in Fig. 5. With the increase of the concentration of H_2O_2, the oxidation peak current of guanine increased gradually till 1.5 mM and then decreased obviously at higher concentration of H_2O_2. It indicated that the maximum activity of HRP was obtained at a concentration of 1.50 mM H_2O_2. This phenomenon could be explained as follows: HRP was activated at a lower concentration of H_2O_2; however, at a higher concentration of H_2O_2, H_2O_2 as an inhibitor reduce the HRP activity [32].

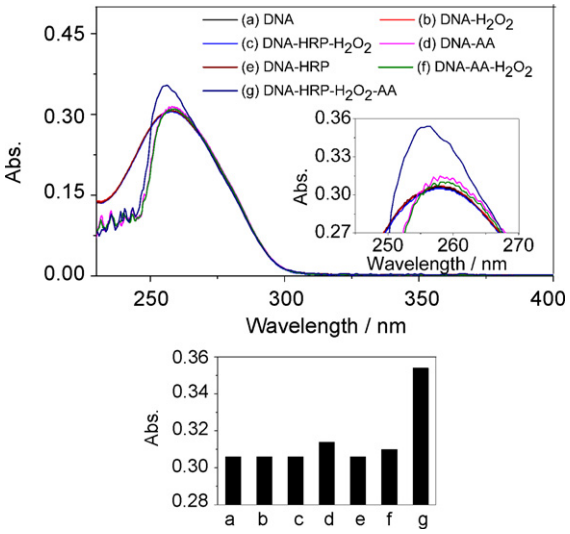

Fig. 6. (A) The UV–vis absorption spectra of 16 μg/mL dsDNA in PBS buffer (pH 7.0) after incubation for 12 h with: (a) blank; (b) 0.5 mM H_2O_2; (c) 1 μg/mL HRP + 0.5 mM H_2O_2; (d) 0.1% AA; (e) 1 μg/mL HRP; (f) 0.1% AA + 0.5 mM H_2O_2; and (g) 1 μg/mL HRP + 0.5 mM H_2O_2 + 0.1% AA. (B) The corresponding histograms.

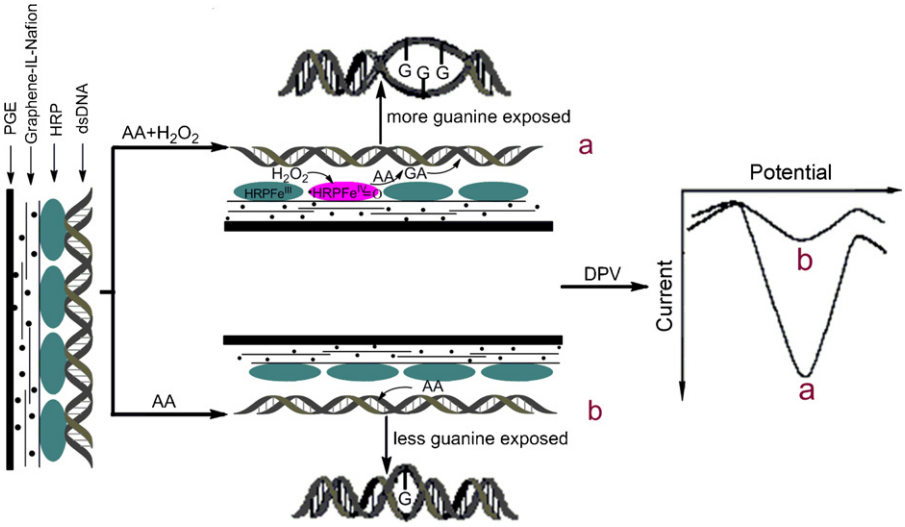

Scheme 2. Schematic diagram of DNA damage induced by AA and glycidamide and the detection method.

3.6. UV–vis spectrophotometric studies on DNA damage induced by AA and its metabolite

In this work, DNA damage induced by AA and its metabolite was investigated in solution by UV–vis spectrophotometry and monitored by the absorbance of DNA at 260 nm. Fig. 6A shows the UV–vis absorption spectra of 16 μg/mL dsDNA in pH 7.0 PBS after incubation with different solutions for 12 h. The UV–vis absorption spectrum of 16 μg/mL dsDNA in pH 7.0 PBS was shown in curve a of Fig. 6A. After incubated with 0.5 mM H_2O_2, 1 μg/mL HRP + 0.5 mM H_2O_2 and 1 μg/mL HRP respectively (shown in curve b, c and e of Fig. 6A, the absorbance of DNA at 260 nm were almost the same as that of curve a. It indicated that H_2O_2, HRP + H_2O_2 and HRP could not induce DNA damage. However, under the existence of 0.1% AA, the absorbance of DNA increased slightly compared with that of curve a, b, c and e in Fig. 6A. Especially, after incubated with 1 μg/mL HRP + 0.5 mM H_2O_2 + 0.1% AA, a significant increase in the peak intensities of DNA at 260 nm companied with an obvious shift to shorter wavelength was observed in curve g of Fig. 6A. This may be explained that during the incubation of DNA with AA or HRP + H_2O_2 + AA, this incubation may disrupt the double-helix of DNA or induce local bulges in the DNA helix, making some additional guanines inside the double-helix structure become exposed, which resulted in the increase of the absorbance of DNA at 260 nm. Furthermore, in order to more vividly present experimental results, the corresponding histograms were also drawn and shown in Fig. 6B.

3.7. Mechanism of DNA damage

In our work, DNA damage induced by AA and its metabolite was investigated at PGE/graphene-IL-Nafion/$(HRP/DNA)_3$ and the possible mechanism of DNA damage was illustrated as follows.

Due to the presence of nucleophilic sites on its purine and pyrimidine bases, DNA was easily attacked by electrophilic reagents. AA with the electron-deficient double bond could form adducts with DNA directly by Michael addition reaction and the reactivity of AA with DNA bases was quite low [33]. These DNA adducts with AA, 1-(2-carboxyethyl)-(2′-deoxyadenosine), N6-(2-carboxyethyl)-(2′-deoxyadenosine), 3-(2-carboxyethyl)-(2′-deoxycytidine) and 7-(2-formamidoethyl)-guanine, may disrupt the double helix of DNA and make additional guanines inside the double helix exposed [34]. It made the exposed guanines oxidized at PGE/graphene-IL-Nafion/$(HRP/DNA)_3$ and DNA damage induced by AA was detected by the guanine signal.

When H_2O_2 was introduced into AA solution, HRP at the modified electrode was activated, which could catalyze the transformation of AA to its epoxide, glycidamide. The relevant reaction equations were listed below:

$$HRPFe^{III} + H_2O_2 \rightarrow HRPFe^{IV}{=}O + H_2O$$

$$^{\bullet}HRPFe^{IV}{=}O + \text{acrylamide} \rightarrow HRPFe^{III} + \text{glycidamide}$$

Due to the higher reactivity of glycidamide with DNA than AA [35], upon formation of DNA–glycidamide adducts, N7-(2-carbamoyl-2-hydroxyethyl)-guanine, N3-(2-carbamoyl-2-hydroxyethyl)-adenine and N1-(2-carboxy-2-hydroxyethyl)-2′-deoxyadenosine, the changes in the double helix of DNA made more additional guanines exposed. Therefore, greater current response for guanine was observed after PGE/graphene-IL-Nafion/$(HRP/DNA)_3$ was incubated with AA + H_2O_2. It indicated that DNA adducts with glycidamide induced more serious DNA damage than AA. In order to clearly show how the biosensor detected DNA damage, the schematic diagram has been drawn and shown in Scheme 2.

To further verify the mechanism of DNA damage, UV–vis spectrophotometry was also used. The absorbance of DNA at 260 nm increased slightly after incubation with AA. However, after incubation with HRP + H_2O_2 + AA, the absorption band of DNA at 260 nm showed obvious increase in the peak intensities (hyperchromic effect). Meanwhile, the band at 260 nm shifted to shorter wavelength. It demonstrated that the double-helix of DNA was disturbed especially after incubated with HRP + H_2O_2 + AA, which resulted in more bases being exposed and the increase in absorbance at 260 nm.

The electrochemical and UV–vis spectrophotometric results indicated that the reaction processes of DNA with AA and HRP + H_2O_2 + AA were different. During the incubation, it was possible that the formation of DNA adducts had the effect of unwinding the double helix, which made additional guanines exposed. Compared with AA, its metabolite produced by HRP/H_2O_2 had a stronger ability to unwind the double helix, which was mainly responsible for DNA damage.

4. Conclusions

In this work, the graphene-IL-Nafion/$(HRP/DNA)_3$ modified PGE was prepared by the layer-by-layer method, which provided an effective strategy for mimicking and detecting DNA damage induced by AA in vivo. The results indicated that under the coexistence of HRP, H_2O_2 and AA, HRP was activated by H_2O_2 and catalyzed the transformation of AA to glycidamide. And the formation of DNA adducts with AA and glycidamide disturbed the double helix of DNA, which made additional guanine inside the double helix of DNA exposed. Based on the changes of guanine signal, DNA damage was directly detected at PGE/graphene-IL-Nafion/$(HRP/DNA)_3$. Moreover, our results also indicated that glycidamide could induce more serious DNA damage than AA, which provided further evidence for the mainly carcinogenic activity of glycidamide. More importantly, this method for directly detecting DNA damage, as a simple and quick means, shows great promise for genotoxicity screening of new chemical pollutants and drugs in vitro.

Acknowledgements

This work was supported by the National Natural Science Foundation of China (No. 21075078) and the Natural Science Foundation of Shandong province, China (No. ZR2010BM005).

References

[1] S. Chevolleau, C. Jacques, C. Canlet, J. Tulliez, L. Debrauwer, Analysis of hemoglobin adducts of acrylamide and glycidamide by liquid chromatography–electrospray ionization tandem mass spectrometry, as exposure biomarkers in French population, J. Chromatog. A 1167 (2007) 125–134.
[2] M. Jagerstad, K. Skog, Genotoxicity of heat-processed foods, Mutat. Res. 574 (2005) 156–172.
[3] E. Tareke, P. Rydberg, P. Karlsson, S. Eriksson, M. Tornqvist, Acrylamide: a cooking carcinogen? Chem. Res. Toxicol. 13 (2000) 517–522.
[4] A. Besaratinia, G.P. Pfeifer, Genotoxicity of acrylamide and glycidamide, J. Natl. Cancer Inst. 96 (2004) 1023–1029.
[5] O.D. Scharer, Chemistry and biology of DNA repair, Angew. Chem. Int. Ed. 42 (2003) 2946–2974.
[6] S.C. Sumner, T.R. Fennell, T.A. Moore, B. Chanas, F. Gonzalez, B.I. Ghanayem, Role of cytochrome P450 2E1 in the metabolism of acrylamide and acrylonitrile in mice, Chem. Res. Toxicol. 12 (1999) 1110–1116.
[7] B.I. Ghanayem, L.P. Mc Daniel, M.I. Churchwell, N.C. Twaddle, R. Snyder, T.R. Fennell, D.R. Doerge, Role of CYP 2E1 in the epoxidation of acrylamide to glycidamide and formation of DNA and hemoglobin adducts, Toxicol. Sci. 88 (2005) 311–318.
[8] I. Maniere, T. Godard, D.R. Doerge, M.I. Churchwell, M. Guffroy, M. Laurentie,.J.M. Poul, DNA damage and DNA adduct formation in rat tissues following oral administration of acrylamide, Mutat. Res. 580 (2005) 119–129.
[9] N. Bistolas, U. Wollenberger, C. Jung, F.W. Scheller, Cytochrome P450 biosensors – a review, Biosens. Bioelectron. 20 (2005) 2408–2423.
[10] L. Zhou, J. Yang, C. Estavillo, J.D. Stuart, J.B. Schenkman, J.F. Rusling, Toxicity screening by electrochemical detection of DNA damage by metabolites generated in situ in ultrathin DNA–enzyme films, J. Am. Chem. Soc. 125 (2003) 1431–1436.
[11] B. Wang, J.F. Rusling, Voltammetric sensor for chemical toxicity using [Ru(bpy)2poly(4-vinylpyridine)10Cl]$^+$ as catalyst in ultrathin films. DNA damage from methylating agents and an enzyme-generated epoxide, Anal. Chem. 75 (2003) 4229–4235.
[12] Y. Zu, N.F. Hu, Electrochemical detection of DNA damage induced by in situ generated styrene oxide through enzyme reactions, Electrochem. Commun. 11 (2009) 2068–2070.
[13] D.W. Potter, J.A. Hinson, Mechanisms of acetaminophen oxidation to N-Acetyl-P-benzoquinone imine by horseradish peroxidase and cytochrome P-450, J. Biol. Chem. 262 (1987) 966–973.
[14] D.H. Yu, B. Blankert, J.M. Kauffmann, Development of amperometric horseradish peroxidase based biosensors for clozapine and for the screening of thiol compounds, Biosens. Bioelectron. 22 (2007) 2707–2711.
[15] M. So, E.G. Hvastkovs, J.B. Schenkman, J.F. Rusling, Electrochemiluminescent/voltammetric toxicity screening sensor using enzyme-generated DNA damage, Biosens. Bioelectron. 23 (2007) 492–498.
[16] D.H. Johnston, K.C. Glasgow, H.H. Thorp, Electrochemical measurement of the solvent accessibility of nucleobases using electron transfer between DNA and metal complexes, J. Am. Chem. Soc. 117 (1995) 8933–8938.
[17] K.S. Novoselov, A.K. Geim, S.V. Morozov, D. Jiang, Y. Zhang, S.V. Dubonos, I.V. Grigorieva, A.A. Firsov, Electric field effect in atomically thin carbon films, Science 306 (2004) 666–669.
[18] H. Chen, M.B. Muller, K.J. Gilmore, G.G. Wallace, D. Li, Mechanically strong, electrically conductive, and biocompatible graphene paper, Adv. Mater. 20 (2008) 3557–3561.
[19] S. Stankovich, D.A. Dikin, G.H.B. Dommett, K.M. Kohlhaas, E.J. Zimney, E.A. Stach, R.D. Piner, S.T. Nguyen, R.S. Ruoff, Graphene-based composite materials, Nature 442 (2006) 282–286.
[20] C.S. Shan, H.F. Yang, J.F. Song, D.X. Han, A. Ivaska, L. Niu, Direct electrochemistry of glucose oxidase and biosensing for glucose based on grapheme, Anal. Chem. 81 (2009) 2378.
[21] L.H. Tang, Y. Wang, Y.M. Li, H.B. Feng, J. Lu, J.H. Li, Preparation, structure, and electrochemical properties of reduced graphene sheet films, Adv. Funct. Mater. 19 (2009) 2782.
[22] M. Zhou, Y.M. Zhai, S.J. Dong, Electrochemical sensing and biosensing platform based on chemically reduced graphene oxide, Anal. Chem. 81 (2009) 5603–5613.
[23] S. Niyogi, E. Bekyarova, M.E. Itkis, J.L. Mc Williams, M.A. Hamon, R.C. Haddon, Solution properties of graphite and grapheme, J. Am. Chem. Soc. 24 (2006) 7720–7721.
[24] J. Li, S.J. Guo, Y.M. Zhai, E.K. Wang, High-sensitivity determination of lead and cadmium based on the Nafion–graphene composite film, Anal. Chim. Acta 649 (2009) 196–201.
[25] G.C. Zhao, M.Q. Xu, J. Ma, X.W. Wei, Direct electrochemistry of hemoglobin on a room temperature ionic liquid modified electrode and its electrocatalytic activity for the reduction of oxygen, Electrochem. Commun. 9 (2007) 920–924.
[26] Y.H. Song, L. Wang, C.B. Ren, G.Y. Zhu, Z. Li, A novel hydrogen peroxide sensor based on horseradish peroxidase immobilized in DNA films on a gold electrode, Sens. Actuators B 114 (2006) 1001–1006.
[27] Y. Li, Y. Wu, Coassembly of graphene oxide and nanowires for large-area nanowire alignment, J. Am. Chem. Soc. 131 (2009) 5851–5857.
[28] J. Li, J.S. Guo, Y. Zhai, Y.E. Wang, High-sensitivity determination of lead and cadmium based on the Nafion–graphene composite film, Anal. Chim. Acta 649 (2009) 196–201.
[29] W. Sun, P. Qin, H.W. Gao, G.C. Li, K. Jiao, Electrochemical DNA biosensor based on chitosan/nano-V_2O_5/MWCNTs composite film modified carbon ionic liquid electrode and its application to the LAMP product of Yersinia enterocolitica gene sequence, Biosens. Bioelectron. 25 (2010) 1264–1270.
[30] F.H. Wu, Z.C. Hu, L.W. Wang, J.J. Xu, Y.Z. Xian, Y. Tian, L.T. Jin, Electric field directed layer-by-layer assembly of horseradish peroxidase nanotubes via anodic aluminum oxide template, Electrochem. Commun. 10 (2008) 630–634.
[31] A.M. Oliveira-Brett, Electrochemistry for probing DNA damage, in: C.A. Grimes, E.C. Dickey, M.V. Pishko (Eds.), Encyclopedia of Sensors, American Scientific Publishers, USA, 2006, pp. 301–314.
[32] A.N.P. Hiner, J. Hernandez-Ruiz, J.N. Rodriguez-Lopez, M.B. Arnao, R. Varon, F. Garcia-Canovas, M. Acosta, The inactivation of horseradish peroxidase isoenzyme A2 by hydrogen peroxide: an example of partial resistance due to the formation of a stable enzyme intermediate, J. Biol. Inorg. Chem. 6 (2001) 504–516.
[33] J.J. Solomon, J. Fedyk, F. Mukai, A. Segal, Direct alkylation of 2′-deoxynucleosides and DNA following in vitro reaction with acrylamide, Cancer Res. 45 (1985) 3465–3470.
[34] D.O. Hull, B. Bajrami, I. Jansson, J.B. Schenkman, J.F. Rusling, Characterizing metabolic inhibition using electrochemical enzyme/DNA biosensors, Anal. Chem. 81 (2009) 716–724.
[35] G. Gamboa da Costa, M.I. Churchwell, L.P. Hamilton, F.A. Beland, M.M. Marques, D.R. Doerge, DNA adduct formation from acrylamide via conversion to glycidamide in adult and neonatal mice, Chem. Res. Toxicol. 16 (2003) 1328–1337.